ORIGINAL ARTICLE

CrossMark

Geochemical mapping of heavy metals around Sukinda–Bhuban area in Jajpur and Dhenkanal districts of Odisha, India

Himadri Bhusan Sahoo[1] · Delwan Kumar Gandre[2] · Prasanta Kumar Das[3] · Mahamad A. Karim[1] · Ganesh Chandra Bhuyan[2]

Abstract

As a part of National Geochemical Mapping (NGCM) programme, regional geochemical mapping was carried out around Sukinda–Bhuban area lying in Jajpur and Dhenkanal districts of Odisha, India. According to the guidelines of NGCM, 698 stream sediment samples were collected at a density of 1 sample per km^2 out of which 179 composite samples were prepared for chemical analysis. An area of about 728 km^2 bounded by latitude 20°45′N–21°00′N and longitude 85°45′E–86°00′E covering toposheet number 73H/13 was surveyed in the year 2013–2014. Elemental baseline geochemical maps were prepared using logarithmic transformation of original concentration values of stream sediment/slope wash samples collected from the study area. Geochemical maps of six heavy metals, viz. Co, Cr, Cu, Ni, Pb and Zn have been produced in this paper and spatial correlations have been found between the underlying geology and element abundances in the sampled media. The northwestern and northeastern parts of the study area contaminated with heavy metals viz. Cr and Ni are also identified which need immediate attention for environmental and societal purposes.

Keywords Geochemical mapping · Stream sediments · Drainage map · Environmental pollution · Sukinda–Bhuban area · Heavy metals · Toposheet

Introduction

Geochemical mapping involves measuring chemical constituents of naturally occurring material on the surface of earth. The study of dispersion pattern of individual elements gives an idea about its source. Geological Survey of India (GSI) has decided to create various sets of baseline geochemical data for the whole country which has resulted in the formulation of National Geochemical Mapping (NGCM) programme since 2001–2002. As a part of this programme, geochemical mapping was carried out for an area of 728 km^2 around Sukinda–Bhuban area covering toposheet number (T.S. no.) 73H/13. The present work is

to prepare a geochemical database which will be helpful in various fields like development of mineral resources, land use, agriculture, forestry, environmental monitoring, various aspects of human and animal health and waste disposal, etc. (Plant et al. 2001; Plant and Hale 1994). In addition, these geochemical data sets demonstrate to agronomists, health and environmental authorities, how geochemical maps produced from stream sediment sampling are useful and effective in delineating regions and targets of relevance to their own specific interests (Licht and Tarvainen 1996; Parsa et al. 2016a, b, c, 2017). The composition of a drainage sediment sample reflects the chemistry of a much wider area than a soil sample so it is a more appropriate sample medium for regional surveys (Appleton and Ridgway 1992).

Sukinda valley was reported as the fourth most polluted place in the world by Blacksmith Institute of the USA (BI 2007). Simultaneously this belt contributes 97% of the country's Chromite ore, a vital component for making stainless steel and alloys and it is one of the largest opencast mines in the world. Air, water and soils are severely contaminated by toxic substances mainly hexavalent Chromium 'Cr (VI)' in and around the chromite mines (BI 2007). A large

✉ Himadri Bhusan Sahoo
silu.himadri@gmail.com

1   Geological Survey of India, State Unit-Karnataka and Goa, Bangalore, India

2   Geological Survey of India, State Unit-Odisha, Bhubaneswar, India

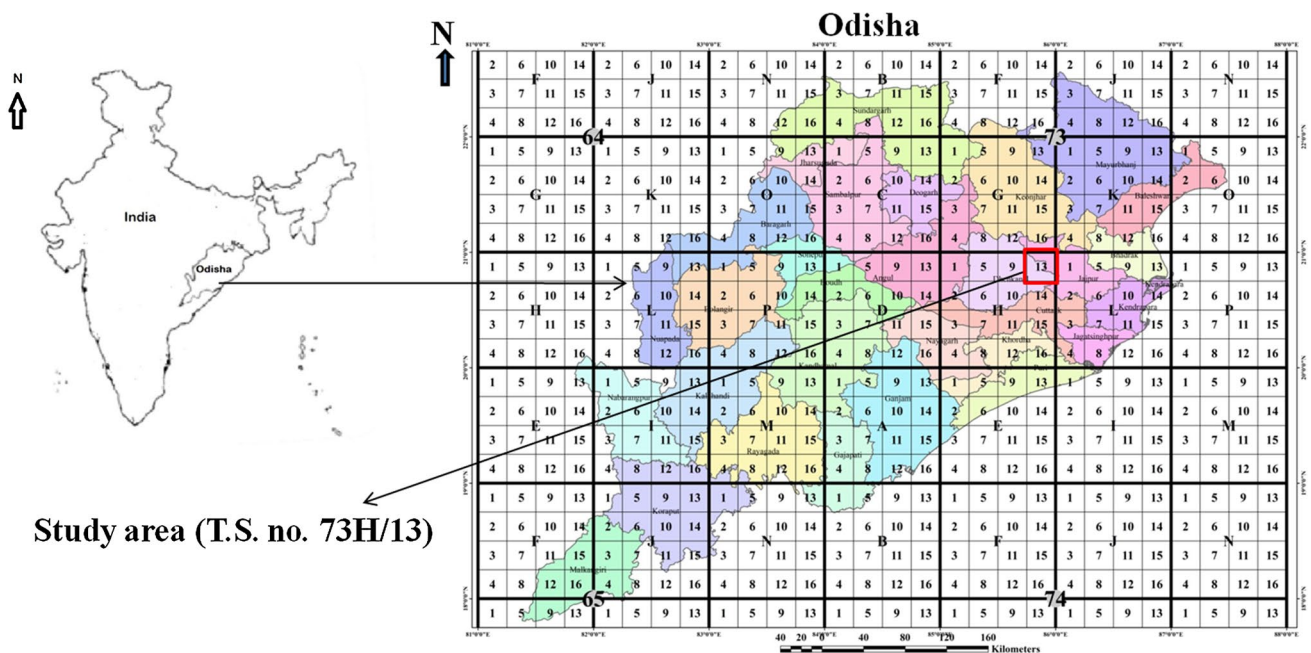3   Geological Survey of India, Central Region, Nagpur, India

Fig. 1 Location map of study area

numbers of studies were carried out on metal contamination in and around Sukinda Chromite mines area falling in T.S. no. 73G/16 and 73G/12 (Pattnaik and Equeenuddin 2016; Das et al. 2013; Samuel et al. 2012; Das and Mishra 2010; Dhakate et al. 2008; Mohapatra et al. 2007). However, available literature on soil heavy metal contamination in the T.S. no. 73H/13 is very limited. Hence, study on both environmentally to access the pollution hazard and economically to find the target Cr ore deposits, if any, in this toposheet is important as it is located near to the chromite mines (south to T.S. no. 73G/16 lying outside of study area) and also in which two major locality Bhuban and Sukinda towns are situated.

Study area

The study area covers Survey of India T.S. no. 73H/13 including parts of Jajpur and Dhenkanal districts of Odisha. The area is bounded by latitude 20°45′N to 21°00′N and longitude 85°45′E to 86°00′E. The location map of the study area is given in Fig. 1. Physiographically, the study area can be divided into three parts, viz. hilly terrain/dense forest (20–25%), plantation/cultivated land (65–70%) and Brahmani River basin area (05–10%). The highest peak is 440 m recorded on the southwestern part of the study area in the Ashwakhola reserved forest. The southwestern and northeastern parts of the toposheet are occupied by high rugged hills of khondalite group and granophyres which are mainly denudational hills. The smaller isolated hills are considered

as residual hills which occur in southeastern and northeastern parts of the area. Most part of the area is occupied by peniplains constituting low-lying areas having flat to gently sloping topography. The area shows an overall dendritic to sub-parallel drainage pattern. General slope in the study area is towards SE and E. Natural springs are present in lateritic country rock. The climate of the study area is humid and sub-tropical and experience normal summer and winter with heavy rainfalls during monsoon. The minimum temperature goes down to about 12 °C during winter, whereas the maximum temperature rises to nearly 39 °C during summer. The area receives an average annual rainfall of 101 cm.[1],[2] The major source of drinking water in the area is ground water, both dug and bore well. For agricultural purposes farmers depend on Brahmani River, major nalas and canals. Soil erosion in the area is mainly caused due to heavy rain during monsoon and anthropogenic activities throughout the year. Almost all the tributaries of Brahmani River are rain-fed which bring tons of soil eroded from upstream. Hence soil erosion is mostly seen along the river banks of the Brahmani River and its tributaries. Apart from the above natural processes, anthropogenic activities also contribute to the soil erosion in the areas having dense population.

The land-use pattern in the study area is mainly controlled by the various geomorphic features/landforms

---

[1] http://jajpur.nic.in/main.htm. Last visited on 26th April, 2017.

[2] http://www.onefivenine.com/india/trace/weatherforecast/Jajapur/Sukinda. Last visited on 2nd May 2017.

developed in the area. Accordingly, the low-lying areas are extensively used for agricultural purpose by the inhabitants. The open scrubs and plateaus in the forest area are generally used for plantation purpose. Northern part is vastly used for cultivation of crops (mainly paddy, vegetables, etc.), whereas southwestern and southern parts are dominated by hilly areas with scattered agricultural land. In areas where laterite is dominant such as in the southwestern and northwestern parts of the area, mining of laterite blocks is used for building material. Unconsolidated lateritic soil (with a local name murom) is used for road construction. Villages are well connected by metalled and unmetalled roads. The rugged hilly terrains are occupied by reserve forests. The southern and northwestern parts of the area are thickly vegetated forming the dense reserved forests (RF) such as Ashwakhola, Sarhangi, Laharha, Raigarha, Bhuban, Dhalaparha, Mahagiri, Barabati and Balibo RF. Among the flora Sal, Shishu, Mahua, neem, Tamarind, Teak, Blackberry, Banyan, Timber, Bamboo, East Indian ebony, Cashew, Acacia and Cactus, etc., are dominant. The main crops of the area are paddy, maize and groundnut. Important fauna present in the area include wild elephants, bear, monkey, wild boar, fox, hyena, deer, snakes, etc.

Geology

The general geology (Srivastava and Mohanty 2005, 2007, 2011) of the study area comprises oldest grit, arkose, conglomerate, metabasics, epidiorite, ferruginous slate, phyllite and banded jasper of Gorumahisani Group of Archaean age mainly occurring in the northeastern part in lenticular forms or irregular patches. Khondalite Group, Charnockite Group, Migmatite Group constituting Eastern Ghat Supergroup of Archaean to Proterozoic age overlie the older rocks. Gneiss of Archaean to Palaeoproterozoic age is represented by garnetiferous granite gneiss, biotite gneiss, tourmaline hornblende gneiss. Dolerite dyke and granophyres of Proterozoic age are the later intrusives. Laterite of Cainozoic age occupies large area in the northwestern and northern part of the toposheet. Quaternary sediments of Pleistocene to Holocene age occupy a major part of the area in the form of low-lying undulating land and form the youngest formation in the area. Occurrence of chromiferous ultramafics have been reported at several places, viz. Kanchanabahali, Bhusal and Chandar areas (Srivastava and Mohanty 2007). The geological map and generalized stratigraphy of the study area (T.S. no. 73H/13) is given in Fig. 2 and Table 1, respectively (modified after MCD 2012; Srivastava and Mohanty 2007).

Sampling techniques

Before initiating the geochemical mapping survey, following pre-field preparations were made. The T.S. no. 73H/13 (1:50,000 scale), aerial photograph, geocoded sheet, soil map and district resource map of the area were studied to understand the general geomorphology, major structural trends, land use and soil cover. The study area was gridded by 1 km × 1 km unit cells as the samples were to be collected from every km^2 area. The toposheet was marked with grids at 2-cm interval (1 km^2) starting from southwest corner of it. The composite samples representing 2 km × 2 km cells have been numbered serially from left to right side and from bottom to top row totalling 182 ± composite cells. Each composite grid comprises four unit cells (1 km^2 each), which are A, B, C and D numbered with prefix of composite sample number (NGCM SOP 2011). The stream sediment and/or slope wash tentative sampling points were marked on drainage map, in advance. Drainage map (Fig. 2) of the sampling area is most essential tool required for planning and executing the geochemical sampling which forms base for preparing distribution maps of various elements analysed. Sample location points in the gridded drainage map superimposed on geological map of the study area are shown in Fig. 3.

For sampling, plastic hand scoops (for scooping sediments), polyethylene bags (carrying samples from field to field camp), stickers for numbering, permanent marker pens of various colours, wooden picks (taking dried mud from the dry stream bed) and portable weighing machine are used. For processing the samples, − 120 mesh nontoxic/ non-contaminating nylon sieves, plastic tub, brush for cleaning the sieves, cloth duster, transparent plastic sheets (spreading and covering wet samples for drying), wooden pestle and mortar (de-lumping mud lumps) and plastic bottles (food grade) of 500 and 250 g capacity (permanent storage of samples) are used. Garmin eTrex 30 GPS (Global Positioning System) for recording of latitude, longitude and elevation (for navigation and for locating the sample points), digital camera for sample point photographs and data sheets (for recording field data at sample sites) are used as essential tools (NGCM SOP 2011).

Stream sediments are mostly represented by fine material (silt-clay) transported by running water. After identifying the sample points in a unit cell, stream sediment samples were collected from 3 to 5 places over a stream stretch of 50–200 m from the 1st- or 2nd-order streams. The stream sediments samples were collected from 0 to 15 cm depth targeting particularly silty and clayey fractions size for sieving (− 120 mesh). If more than one 1st-order stream is originating in a cell and extending into adjacent cells, the longest stream covering relatively large

LEGEND

Q_3p	Sand, silt, clay	Present day deposit
Q_2b	Sandy clay	Banklgarh Formation
$Q_{12}f$	Compact clay with caliche nodules.	Fategarh Formation
Q_1b	Lateritised soil	Bolgarh Formation
Czl	Laterite	
?Pt	Granophyre	
βPtd	Dolerite	
	Garnetiferous granite gneiss	Paninsular gneiss
APteggn	Granite gneiss	Migmatite Group
APtegc2	Acid Charnockite	Charnockite Group — Eastern Ghat Supergroup
APtegc1	Basic Charnockite	
APtegk2	Calc granulite	Khondalite Group
APtegk3	Quartzite	
APtegk1	Quartz-garnet-sillimanite graphite schist gneiss	
Ag4	Banded Jasper	Gorumahisani Group
Ag3	Ferruginous slate, phyllite	
Ag2	Meta basic rock, epidiorite	
Ag1	Grit, arkose, conglomerate	

STRUCTURAL SYMBOLS

Foliation: Inclined

Joint: Vertical   Geological Contact

GEOMORPHOLOGICAL SYMBOLS

Point bar/ Channel bar   WB   Water body

Stabilised bar   Major road

INDEX

River   Drainage
Stream   Settlement
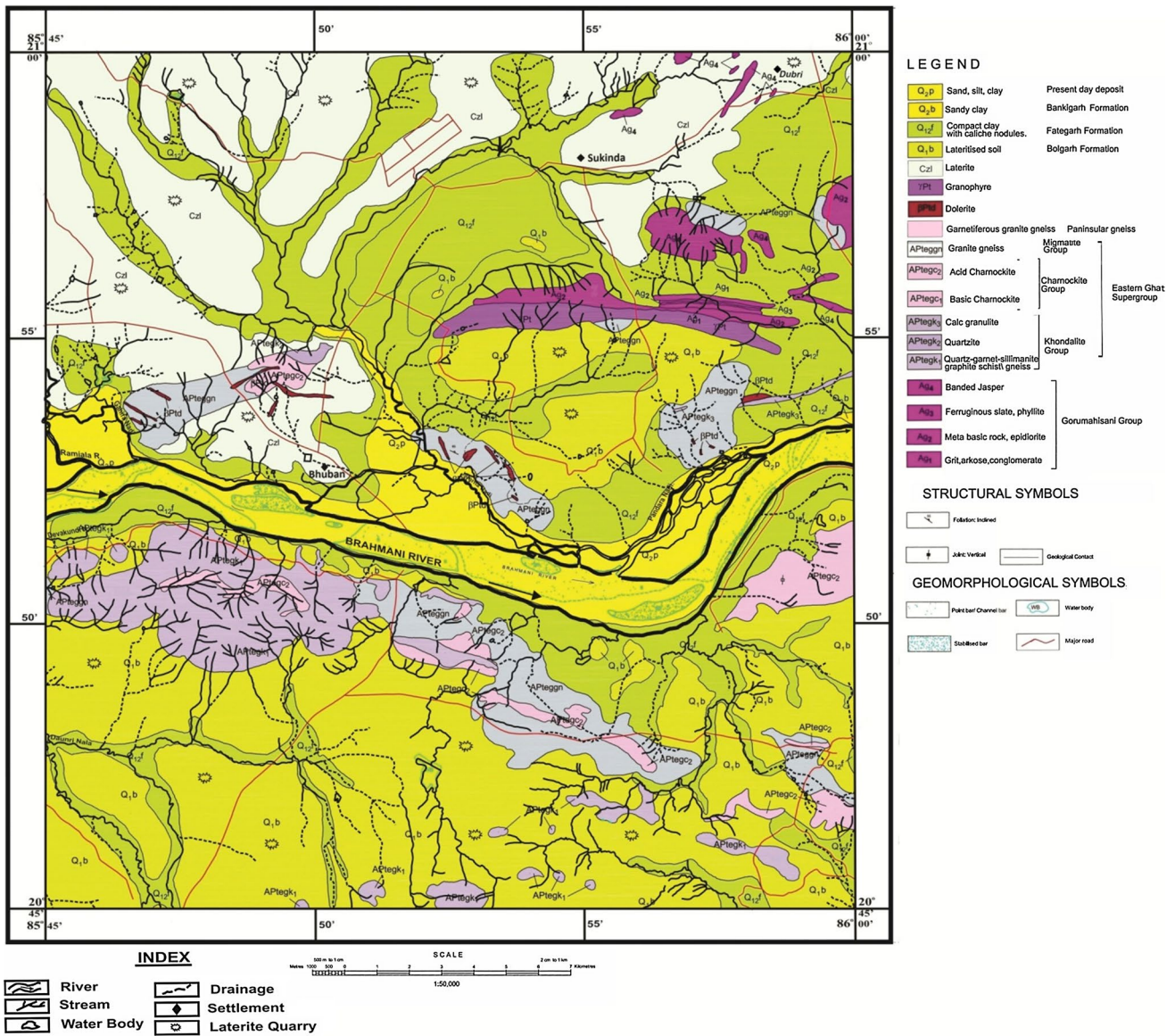Water Body Laterite Quarry

SCALE
1:50,000

Fig. 2 Drainage map superimposed on geological map of the study area

basin area of its own is selected on site and sampling done near the exit point of the stream within the unit cell. If two or more first-order streams confluence within the cell, the site below the confluence and just above the edge of the unit cell is sampled. In case drainage is absent in a unit cell, slope wash material generated by gully erosion has been collected considering it to be a 'zero' order stream. Such samples are usually collected from three to five places of the slope from regolith (0–15 cm after removing the top humus material if any) to make a representative sample of that unit cell. Dried samples were sieved at the sample location using − 120 nylon sieves. For wet samples, about 4–5 kg of raw sample of stream sediment/slope wash material (depending up on the nature of sediment) were collected from each cell and brought to the field camp in thick polythene bags (Fig. 4). As per the guidelines (NGCM SOP 2011), at each unit cell sampling point, site specific information such as surrounding geology, lithounits exposed, slope, order of stream, nature of sediment, channel character, health hazard, land use, mineralization, contamination, sampling site co-ordinates and elevation, etc., were collected in the field data sheet. Figure 5 shows some of the rocks of economic importance observed in the study area during field work.

In the field camp, the wet samples collected were sun-dried in thick transparent plastic sheets. Then the sun-dried stream sediment/slope wash samples were processed and sieved through − 120-mesh nylon cloth after de-lumping

Table 1 Generalized stratigraphy of the study area

Rock type	Formation	Group	Supergroup	Age
Sand, silt, clay	Present day deposit	–	–	Quaternary
Sandy clay	Bankigarh Formation			
Compact clay with caliche nodules	Fatehgarh Formation			
Lateritised soil	Bolgarh Formation			
Laterite				Cainozoic
Quartz vein, dolerite, pink granite, granophyre, chromiferous ultramafic	Intrusive	–	–	Proterozoic
Garnetiferous granite gneiss, banded gneiss, augen gneiss	–	Migmatite Group	Eastern Ghat Supergroup	Archaean to Proterozoic
Pyroxene granulite, charnockite	–	Charnockite Group		
Calc granulite quartzite, quartz–garnet–sillimanite–graphite schist/gneiss	–	Khondalite Group		
Tectonic contact				
Quartzite, banded jasper ferruginous slate, phyllite, metabasic rock, epidiorite, grit, arkose, conglomerate, banded chert, meta-ultramafic	Volcano meta-sedimentary sequence	Gorumahisani Group	Iron ore Supergroup	Archaean
Base not exposed				

with a wooden mallet; 500 g sample were collected after homogenization (Fig. 4). Sufficient care has been taken to avoid contamination during sampling in field and preparation by coning and quartering method for storage and analysis. These samples were made into two parts of 250 g each, out of which one is preserved in the plastic container and stored as field reference sample for the respective unit cell. The remaining 250 g samples from four adjacent unit cells are mixed together and homogenized to form a composite sample and then split into two samples of 500 g each by coning and quartering (Fig. 4). One of it is stored as duplicate samples for future reference and the other is sent to chemical laboratory for chemical analysis. The samples are stored in non-toxic, non-contaminating plastic bottles (Tarson 250 and 500 ml) and labelled with stickers. The flow chart of NGCM sampling from pre-field preparation to sample storage plan is illustrated in Fig. 6.

Chemical analysis and quality control

All the samples were analysed by GSI laboratory located at Chemical Division, Eastern Region, Kolkata, India. According to the requirements, XRF (X-ray fluorescence) Spectrometer was adopted to analyse the six heavy metals of interest discussed in the paper. The XRF instrument used in this analysis is PANalytical MagiX 2424 WD XRF spectrophotometer with a rhodium end window X-ray tube operated at 2.4 KW. This instrument is a sequential wavelength dispersive X-ray fluorescence spectrometer with a single goniometer-based measuring channel, covering the

complete measuring range and microprocessor controlled for maximum flexibility. The whole system is controlled from an external computer, running an analytical software package (SuperQ). The elements of interest were analysed by pressed pellet method (XRF SOP 2010). Quality/reproducibility was checked by introducing duplicate samples after a batch of every 10 samples and accuracy was measured by introducing SRM (standard reference material) samples in each batch of 20 Samples (XRF SOP 2010). Internationally recognized standard reference material of GSD (GSD-1 to 9) and STSD (STSD-1 to 4) series were used for chemical analyses (Darnley et al. 1995). The detection limits of the elements of interest are furnished in Table 2.

Geochemical mapping and processing of data

This project had been taken up under NGCM programme to generate high-density multi-purpose geochemical database for 68 elements in stream sediment/slope wash material. The sampling was carried out in 1 km × 1 km cells (Zhizhong et al. 2014). All samples are analysed for 68 elements using 'clark' as the lower level of detection. In certain cases, the detection levels may be lower than clark (NGCM SOP 2011). The details of chemical analysis and the instruments used are given in NGCM SOP (2011). Thus, NGCM generates true national and regional geochemical data sets by fulfilling several criteria (Smith et al. 2013).

In this paper, the analytical values of six heavy metals were taken for statistical analysis as well as for preparing
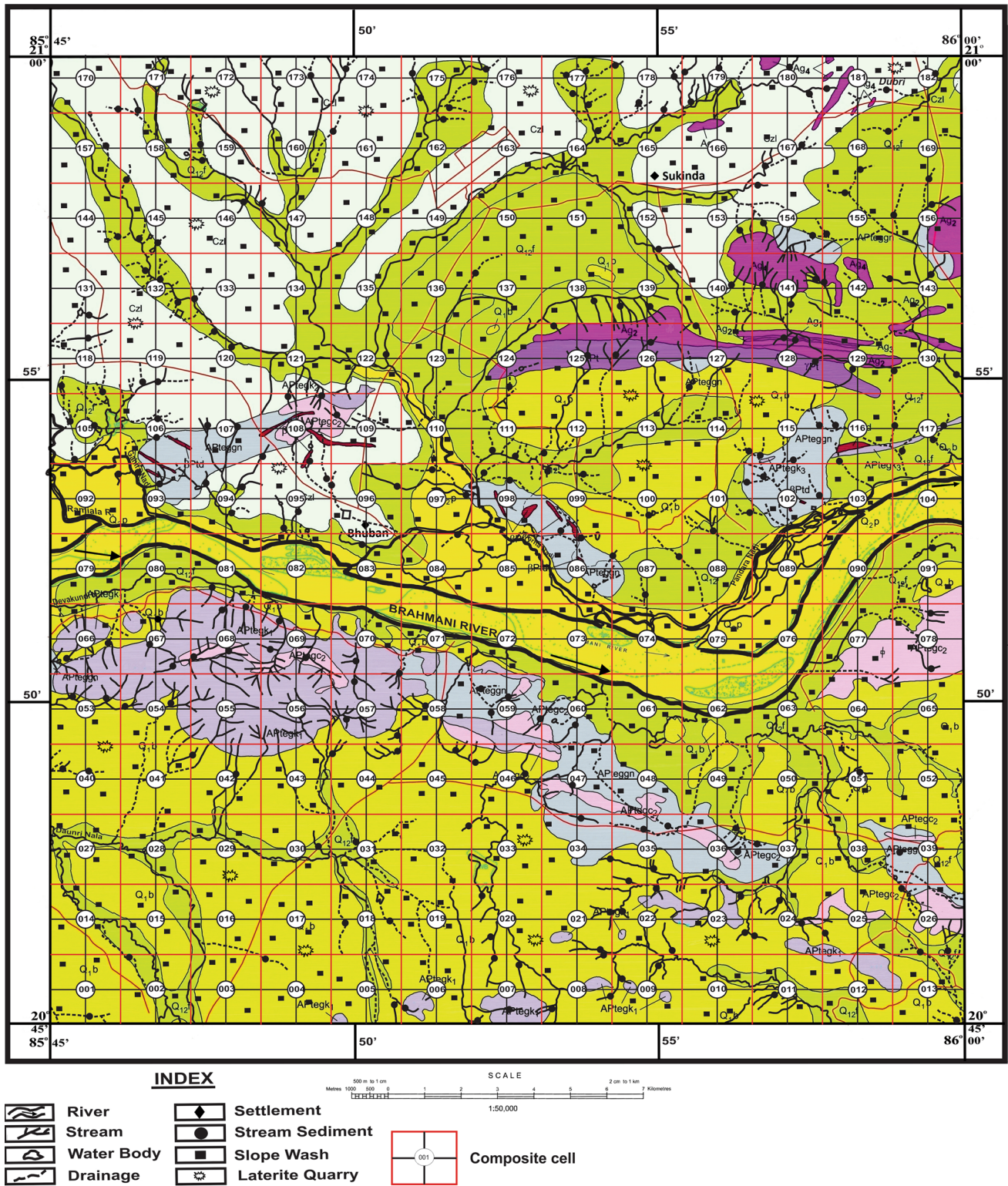
Fig. 3 Gridded geological map of the study area showing sample location points. For lithounits refer Fig. 2

geochemical maps. All statistical analyses were done by Microsoft excel 2007 and Statistica, and contour diagrams were prepared by using Surfer 12 software. The contour

diagrams of elemental distribution are superimposed on various maps, viz. geological map for interpretation in terms of geology, mineralogy, agriculture and environmental aspects.

Fig. 4 Photographs showing procedure from collection of geochemical sample to preparation of sample for chemical analysis. **a** Collection of stream sediment sample (unit cell sample) from a stream in the study area. **b** Sun drying of collected unit cell samples by putting in transparent polythene sheet at the field camp. **c** Sieving of dried unit cell samples through − 120 mesh sieve and subsequent storage of sample in zipper polythene in the field camp. **d** Preparation of composite cell samples by through mixing of unit cell samples followed by coning and quartering and weighing. Finally, samples are stored in labelled bottles for chemical analyses and future reference
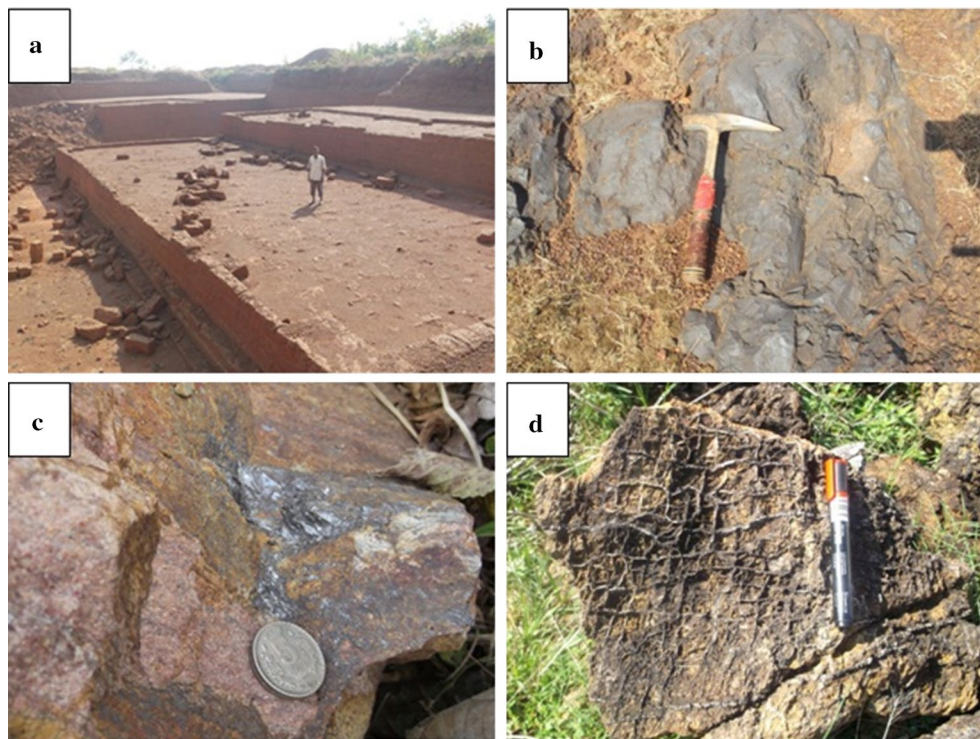
Fig. 5 Various rocks of economic importance observed in the study area. **a** Working laterite quarry, **b** banded iron formation, **c** graphite in khondalite, **d** chromiferous ultramafics
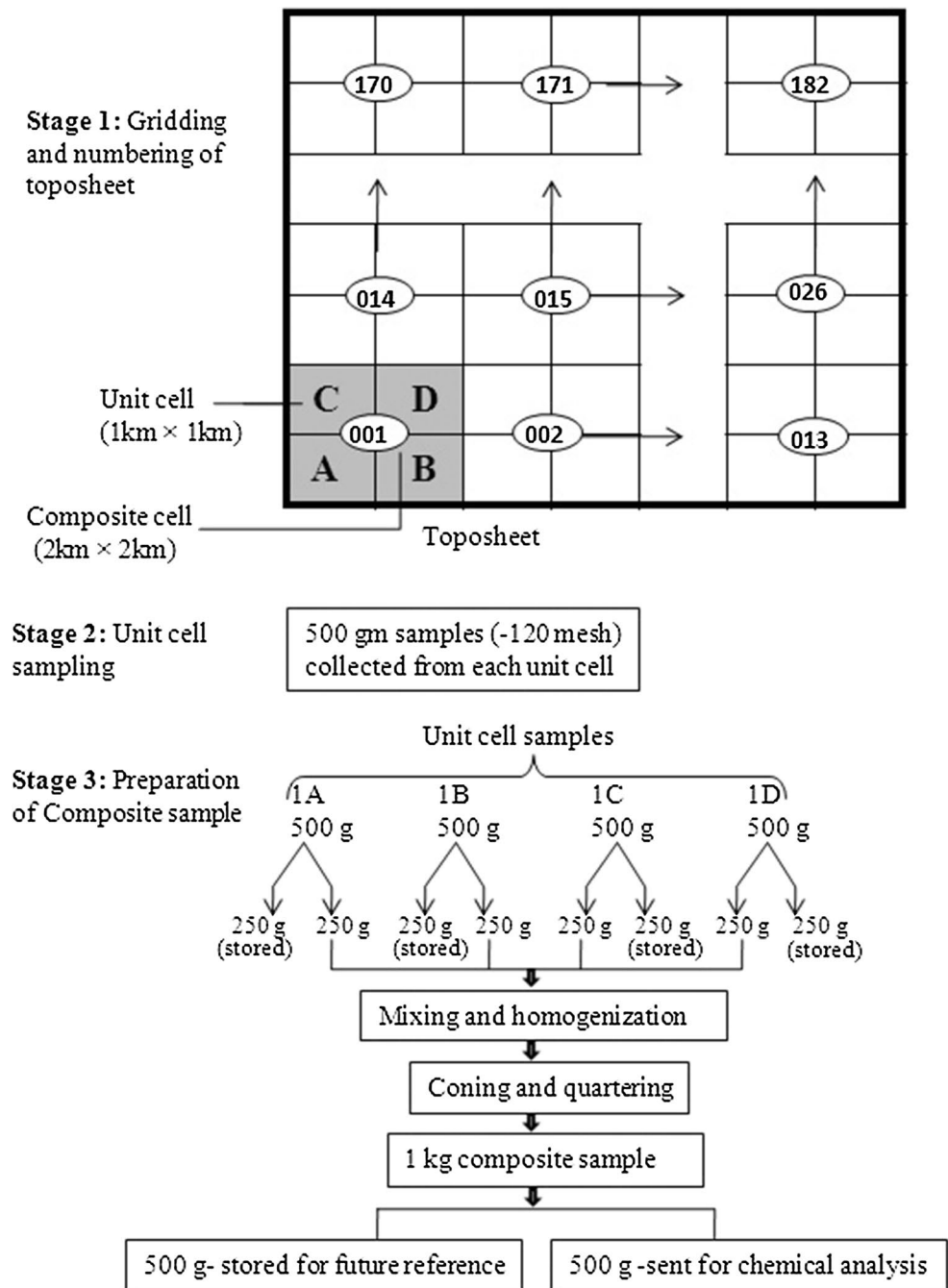
Fig. 6 Flow chart for geochemical sample preparation

Element	Co	Cr	Cu	Ni	Pb	Zn
Detection limit (ppm)	1	15	1	2	2	10

Statistical parameters and contour diagrams have been prepared from the analytical results of different elements for the composite stream sediments/slope wash samples. The statistical parameters (Table 3), viz. mean, median, mode, standard deviation, etc., were computed and studied along with the distribution pattern as depicted in the geochemical maps. Mean and median give a measure of central tendency. Standard deviation gives a measure of statistical dispersion. Reimann et al. (2005) concluded that for real geochemical data, the rule of [mean $\pm$ 2 standard deviation (STDV)] is less appropriate compared to the [median $\pm$ 2 median absolute deviation (MAD)]. In this study, median value for

Table 3 Values of statistical parameters calculated for different elements (in ppm)

Parameters	Co	LogCo	Cr	LogCr	Cu	LogCu	Ni	LogNi	Pb	LogPb	Zn	LogZn
Mean	26.251	1.37024	635.112	2.54887	37.039	1.54543	62.446	1.69619	27.357	1.42450	51.843	1.69649
Median	23	1.36172	256	2.40823	34	1.53147	43	1.63346	26	1.41497	49	1.69019
Mode	18	1.25527	162	2.20951	35	1.54406	38	1.57978	24	1.38021	41	1.61278
Standard deviation	13.119	0.20565	948.031	0.41716	13.367	0.13742	62.681	0.25674	6.880	0.10350	15.546	0.12516
Variance	172.133	0.04229	898762.7	0.17403	178.701	0.01888	3929.01	0.06591	47.343	0.01071	241.694	0.01566
Kurtosis	1.535	− 0.29811	11.307	0.22440	3.216	0.55991	27.233	2.07353	3.187	0.21891	1.416	− 0.22837
Skewness	1.257	0.11010	3.204	1.04164	1.677	0.67764	4.541	1.33581	1.211	0.30184	0.987	0.17742
Range	72	1	5559	1.69690	76	0.73803	532	1.42050	46	0.58827	93	0.66057
Minimum	8	0.90309	114	2.05690	17	1.23044	21	1.32221	16	1.20412	26	1.41497
Maximum	80	1.90309	5673	3.75381	93	1.96848	553	2.74272	62	1.79239	119	2.07554
Number of samples	179	179	179	179	179	179	179	179	179	179	179	179
MAD	10.378	0.19463	169.016	0.35719	8.895	0.12501	19.273	0.19267	5.930	0.09214	13.343	0.11958
Threshold value	43.756	1.75099	594.032	3.12262	51.791	1.78150	81.547	2.01882	37.860	1.59925	75.686	1.92935

each element is taken as the background concentrations and median plus two times the median absolute deviation (MAD) is taken as the 'threshold value' above which anomalous concentration of element is considered. The reason behind considering [median ± 2 MAD] over [mean ± 2 STDV] is because of the robustness and appropriateness of the former for non-normal data (Adekeye 2012). MAD values are determined by using below equation (modified after Leys et al. 2013; Adekeye 2012).

$$MAD = b\big[\text{Median}(|X_i − M(X_i)|)\big]$$

where X_i is the individual observations in the given data set and $M(X_i)$ is the median of the data set. $b = 1.4826$, a constant linked to the assumption of normality of the data, disregarding the abnormality induced by outliers.

The divisions made in the contour maps are based on median, median ± MAD and median + 2MAD, and the contour interval is 0.05.

Distribution of elements and statistical tests

Anomalous zones of higher elemental concentration could help in demarcating targets related to mineral deposits, to urban and/or industrial wastes, to pesticide application, contaminated zones (land, water or air) to some specific diseases and regions with lower elemental concentration could be helpful in delineating targets related to some particular rock types characterized by low primary concentrations or epigenetic/ supergene depletion, or in assessing crop productivity or the occurrence of some specific diseases (Licht and Tarvainen 1996). It would be advantageous to all concerned if geochemical data and samples obtained by industry could be made available with the appropriate government agency

to ensure the maximum possible use of the results in the national interest (Webb 1975).

The distribution maps were superimposed over the geological map of the area for the easy interpretation of the elemental distribution pattern. Distributions of cobalt (Co), chromium (Cr) copper (Cu), lead (Pb), nickel (Ni) and zinc (Zn) show positively skewness indicating presence of a tail deviating from normal distribution towards higher values and a logarithmic transformation tends to move their skewness towards normality, i.e. closer to 0 (Zhang et al. 2005). So histograms are plotted after normalization (log transformation) of the data sets for each element to reduce positive skewness. The data are used to create interpolated contour maps of each element by using Surfer software. Krigging method of interpolation is used for preparing the contour maps.

Histograms and Q–Q plots (by STATISTICA) were generated to test the normal distributions of the data sets of each element which are shown in Figs. 7 and 8, respectively. Histograms and Q–Q plots of the elements of interest fit with the normal distribution except at the higher values. The normality tests are supplementary to the visual assessment of normality (Elliott and Woodward 2007). The tests for the assessment of normality of the data after log transformation was carried out by various tests, viz. Shapiro–Wilk test, Anderson–Darling test, Lilliefors test, Jarque–Bera test and Kolmogorov–Smirnov test (Ghasemi and Zahediasl 2012) using XLSTAT add-in with the MS excel 2007. The results for the above-mentioned tests are given in Table 4. Among these, Shapiro–Wilk test is considered as the best choice for testing normality of data (Ghasemi and Zahediasl 2012). It is clear from the results of Shapiro–Wilk test (Table 4), the p values of Co, Pb and Zn are greater than the alpha value ($\alpha = 0.05$) which indicate normal distribution of the data while the p values of Cr, Cu and Ni are lesser than the alpha
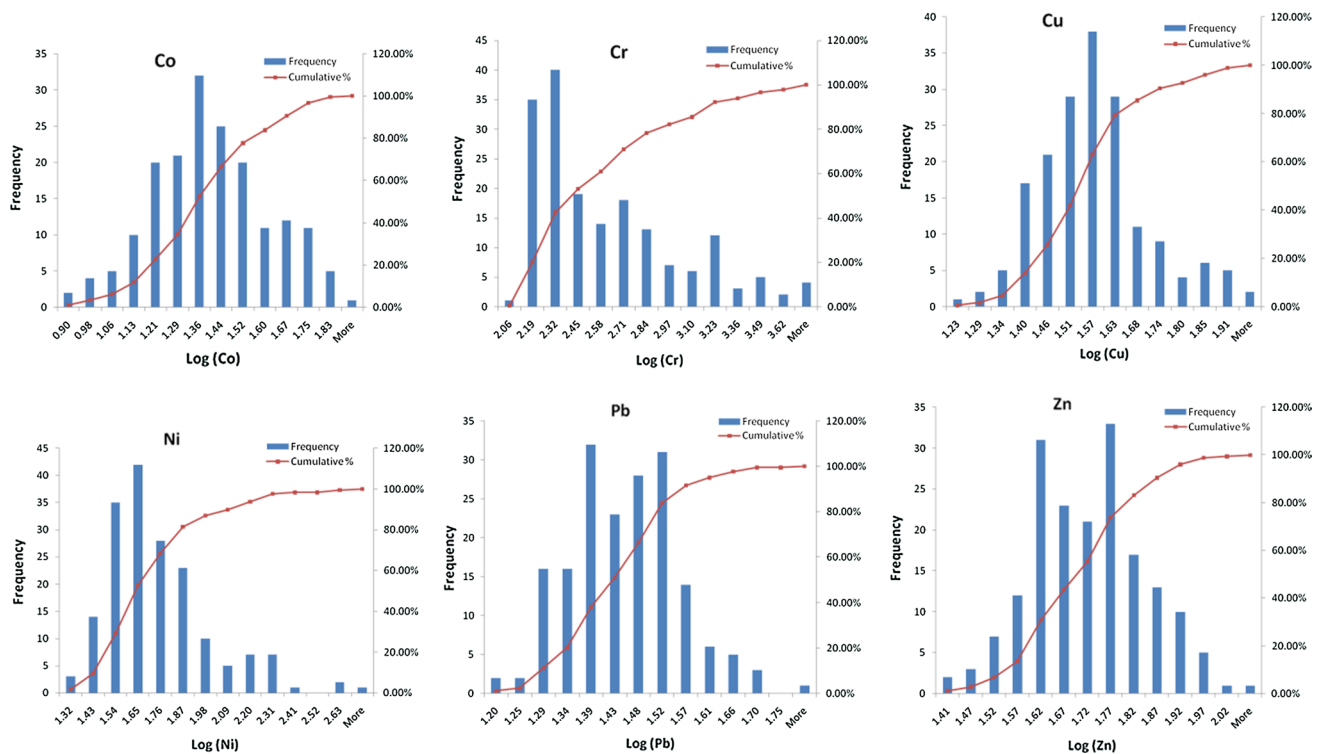
Fig. 7 Histograms for the six heavy metals

value indicating a non-normal distribution of data. According to the results obtained from Kolmogorov–Smirnov test, except Cr and Ni other four element data (Co, Cu, Pb, Zn) show normal distribution. True normality is considered to be a myth (Elliott and Woodward 2007) and hence normality should be tested visually by using normal plots (Ghasemi and Zahediasl 2012; Field 2009). For large sample sizes (> 30 or 40), the violation of the normality assumption should not cause major problems (Pallant 2007) and the sampling distribution tends to be normal, regardless of the shape of the data (Field 2009; Elliott and Woodward 2007). The visual assumptions of data from histograms and Q–Q plots of the six elements do not show serious deviation from the normality. Reimann and Filzmoser (2000) stated that regional geochemical data practically never show a normal distribution. From the above discussion, i.e. normality test, visual plots and large nos. of data (*n* = 179), the data for six heavy metals can be considered as normally distributed.

Correlation matrix of these six heavy metals was calculated and furnished in Table 5. The correlation matrix is an important measure of linear association between two variables in a manner not influenced by the measurement units. The correlation is more useful as a measure of association between two random variables than the covariance.

The principal component analysis (PCA) and cluster analysis has been used to understand the source of metals (Odokuma-Alonge1 and Adekoya 2013; Yap 2012; Morrison et al. 2011; Templ et al. 2008). The principal component analysis is carried out by using SPSS software. The cluster analysis is carried out through dendrogram that is prepared by Ward link method using Minitab software.

Heavy metals of interest for study (Co, Cr, Cu, Ni, Pb and Zn)

Correlation matrix study indicates a strong positive correlation (*r* = 0.65–0.85) of Co with Cu and Zn while moderately strong correlation (*r* = 0.5–0.65) of Co with Ni. Cr shows strong positive correlation with Ni and negative correlation with Pb and Zn. Cu shows a strong positive correlation with Zn.

The PCA analysis was performed using concentration values of Co, Cr, Cu, Ni, Pb and Zn after logarithmic transformation for understanding their controlling factors. Two factors were extracted corresponding to Eigen value > 1, and they explain 71% of the total variance. Varimax rotated factor loading are given in Table 6. For interpreting a group of variables associated with a particular factor, loading > 0.6 was considered. The first factor (PCA1) describes 44.6% of the variance and is strong positive loading with Co, Cu and Zn. This indicates that these three metals have similar behaviour and probably derived from a common source. The second component
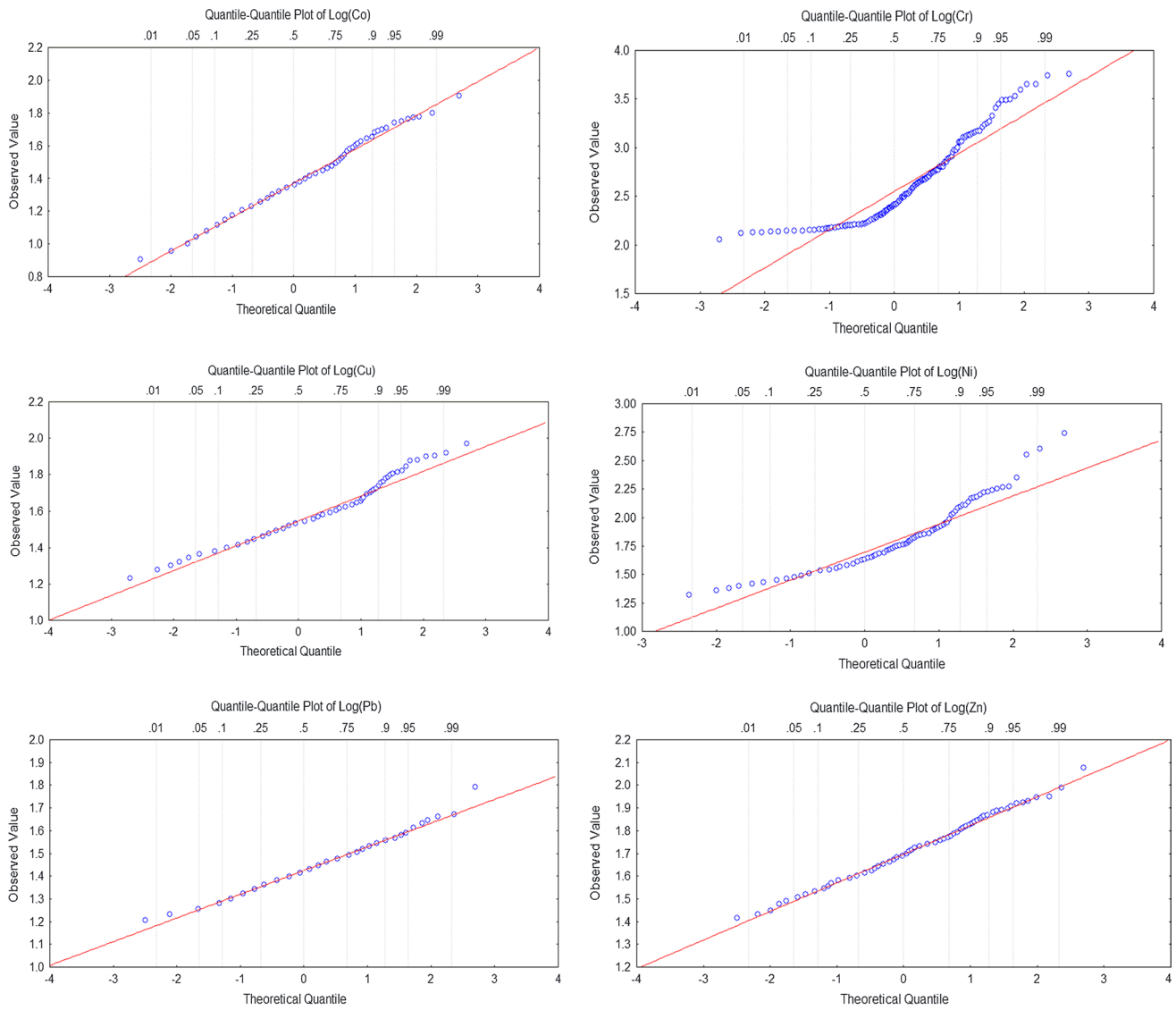
Fig. 8 Q–Q plot for the six heavy metals

Table 4 Results of normality tests for the six heavy metals

Variable\test	Shapiro–Wilk ($\alpha = 0.05$)		Anderson–Darling ($\alpha = 0.05$)		Lilliefors ($\alpha = 0.05$)		Jarque–Bera ($\alpha = 0.05$)		Kolmogorov–Smirnov ($\alpha = 0.05$)	
	p value	Statistic (W)	p value	Statistic (A^2)	p value	Statistic (D)	p value	Statistic (JB)	p value	Statistic (D)
Log Co	0.239	0.990	0.196	0.509	0.265	0.053	0.567	1.153	0.695	0.052
Log Cr	< 0.0001	0.870	< 0.0001	7.634	< 0.0001	0.145	< 0.0001	32.083	0.001	0.144
Log Cu	0.00019	0.965	0.000	1.806	0.003	0.085	0.000	15.419	0.145	0.085
Log Ni	< 0.0001	0.898	< 0.0001	4.962	< 0.0001	0.124	< 0.0001	81.664	0.007	0.124
Log Pb	0.12498	0.988	0.341	0.410	0.438	0.047	0.233	2.913	0.820	0.046
Log Zn	0.49872	0.993	0.388	0.386	0.197	0.055	0.494	1.410	0.607	0.056

α = level of significance

Table 5 Correlation matrix of six heavy metals

Elements	LogCo	LogCr	LogCu	LogNi	LogPb	LogZn
LogCo	1					
LogCr	0.11042	1				
LogCu	0.69662	0.23223	1			
LogNi	0.58384	0.67464	0.61737	1		
LogPb	0.30771	− 0.34746	0.08323	− 0.15098	1	
LogZn	0.68579	− 0.06226	0.66289	0.34216	0.35765	1

Table 6 Factor loading rotated matrix for six heavy metals

Metals	Component	
	PCA 1	PCA 2
Co	0.884	0.109
Cr	0.089	0.853
Cu	0.822	0.117
Ni	0.528	0.731
Pb	0.360	− 0.603
Zn	0.844	− 0.159
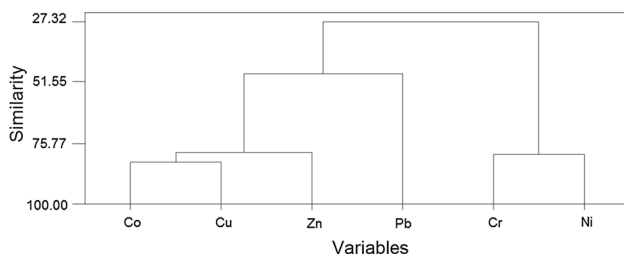
Fig. 9 Dendrogram showing results of hierarchical clustering of the six heavy metals

(PCA2) describes 26.4% of the variance and is highly positively loaded with Cr and Ni, and negatively with Pb which implies possible derivation from same source type, i.e. ultramafics parentage. The ultramafic source is further substantiated by the presence of Sukinda ultramafic complex (located upstream outside of the study area) containing significant quantity of stratiform chromite deposit and nickeliferous laterite (Pattnaik and Equeenuddin 2016) and chromiferous laterite in the study area. The dendrogram obtained after cluster analysis is shown in Fig. 9. It also favours very close association of Cr and Ni and similar behaviour with each other while Cu, Co and Zn form another cluster.

The contour map of Co (Fig. 10) shows medium to higher values (40–80 ppm) in northeastern part located over the Gorumahisani Group of rocks and laterite. Two isolated patches of higher Co anomalies occur in southern and western parts over the granite gneiss (Migmatite Group) and lateritic terrain. All other parts of the map show Co values less than 35 ppm.

The higher concentration values of Cr exceeding the threshold value (> 594 ppm) are seen in patches as local anomalies in the northwestern and northeastern part of the area located over the lateritic country rock (Fig. 11). Local Cr anomalous zone in the northwestern part of the study area may be attributed to secondary enrichment of chromium from the Sukinda chromite mines situated northwestern side of the study area whereas the eastern anomalous zone indicates more towards the presence of primary source rich in chromium (ultramafic rocks) underneath or near to the surface. The presence of small kinks or changes of slope (for higher concentration values of Cr) in the Q–Q plot of Cr (Fig. 8) also suggests the presence of different sets of populations for the Cr concentration data. Some extreme concentration values appear as separated from the majority of the samples mainly for Cr and Ni, i.e. they do not appear to be part of a continuous distribution in the Q–Q plot (Fig. 8). These high values are termed as outlier and in exploration geochemistry might be considered as evidence of mineralization or other rare processes (Zhang et al. 2005). However, high concentrations of elements, viz. Cr, Ni, Pb, Zn, etc., can also be influenced by anthropogenic pollution like mining activities, use of agricultural manure, untreated industrial disposals/effluents etc. In addition, anomalous zone of higher concentrations of Ni (> 81 ppm) is observed in the northwestern and northeastern part of the map over lateritic rocks exposed (Fig. 12) in that area indicating the possible occurrence of mafic and ultramafic body in the northwestern/northeastern part of the study area. From the correlation matrix table, positive correlation between Cr and Ni favours the congenial milieu of the presence of ultramafic body from which they might have been derived particularly in the eastern part of the study area. Chromium concentration exceeds safe limit (Table 7) in the northwestern and northeastern part of the study area alarming health authorities to act accordingly. High pronounced isolated anomalous values of Cr and Ni found in northwestern and northeastern parts which may be influenced by chromiferous rich laterites or by pre-existing mines/steel plants in the vicinity, need detailed investigation works in the respective two zones to address the issue precisely.

The contour map of Cu (Fig. 13) superimposed on geological map shows higher values in northeastern parts
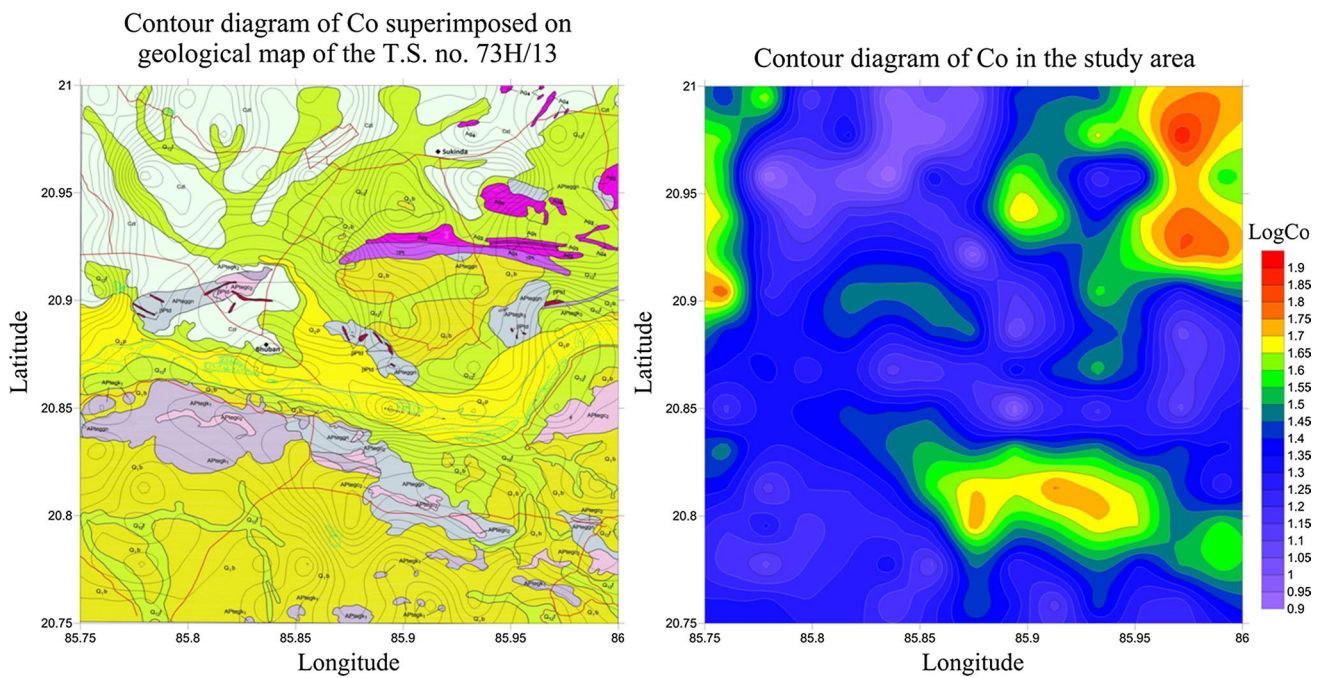
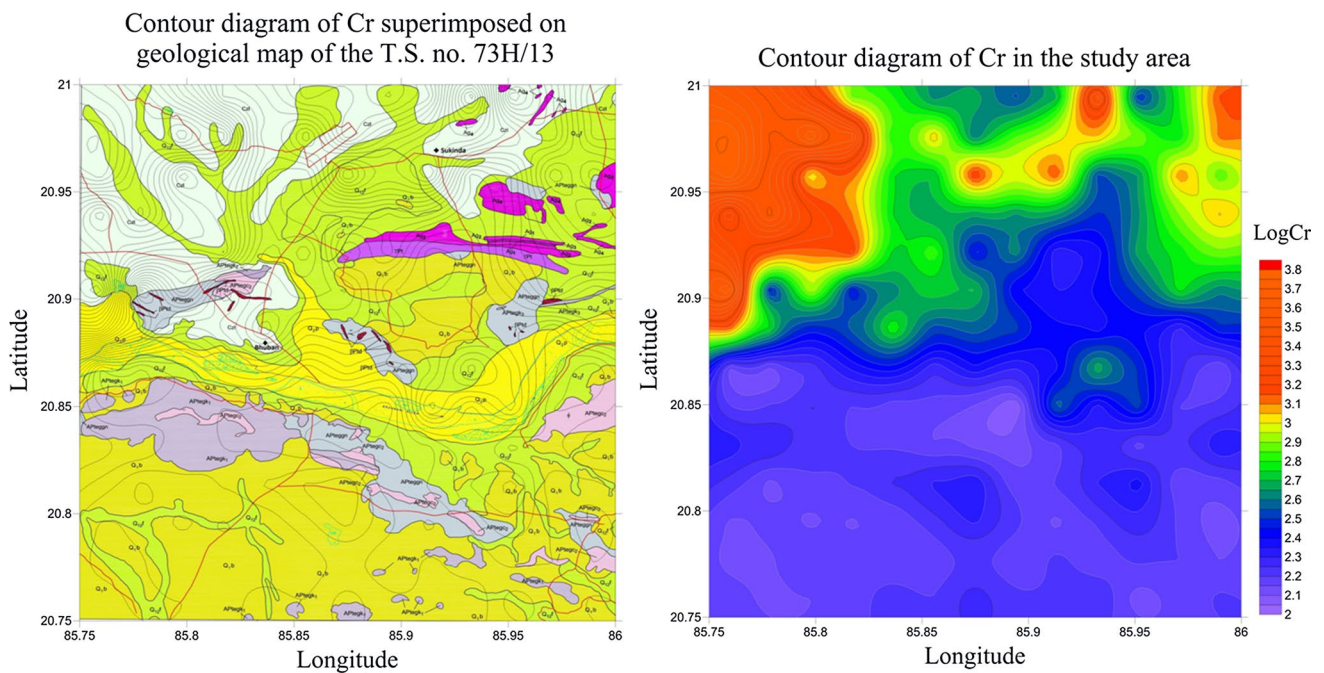**Fig. 10** Contour diagram of Co in the study area

Fig. 11 Contour diagram of Cr in the study area

of the total area over the Gorumahisani Group of rocks and laterite. The background concentration values of Cu, i.e. below threshold values (< 51 ppm) occur in the lateritic soil and quaternary sediments. Nickel and Cu are essential elements for plant (Micó et al. 2006). But the concentrations of Ni and Cu show values less than 100 and 140 ppm, respectively, throughout the area except northwestern and northeastern parts. Hence, these areas require external nourishment for increased crop productivity in the agricultural lands.
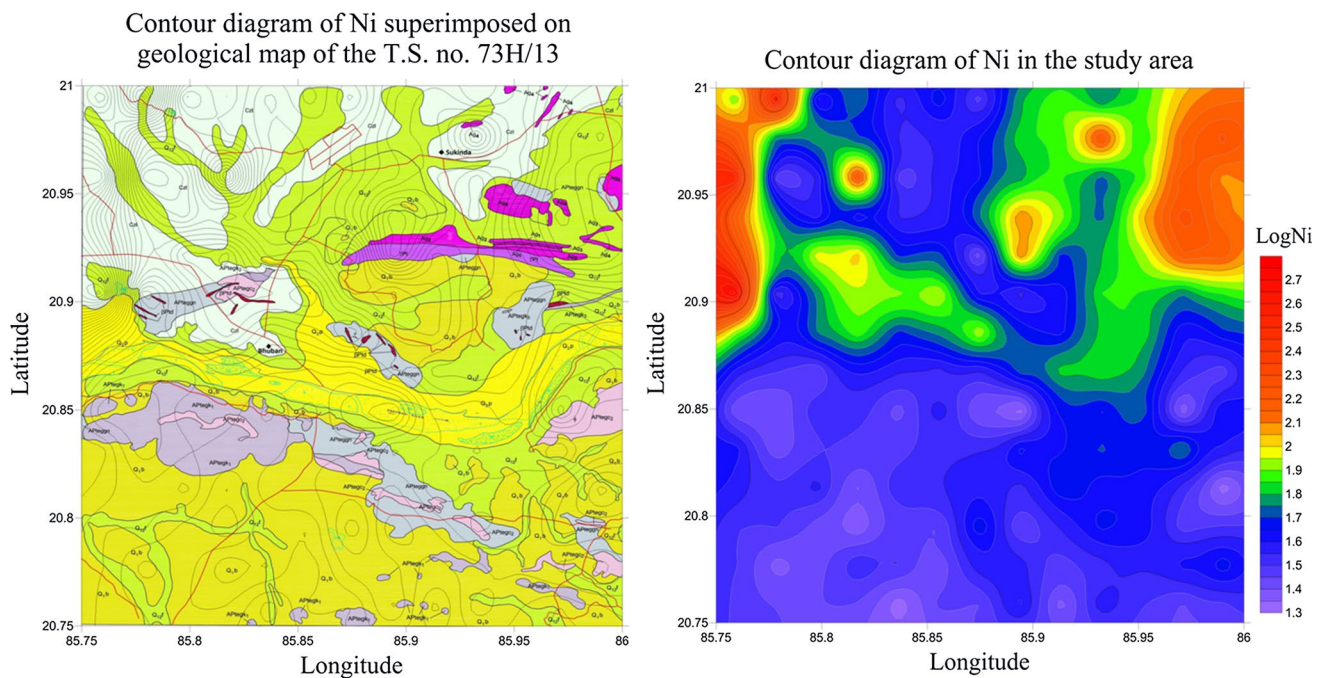
Contour diagram of Ni superimposed on
geological map of the T.S. no. 73H/13

Contour diagram of Ni in the study area

Fig. 12 Contour diagram of Ni in the study area

Table 7 Values of maximum permissible limit of heavy metals in μg/g of dry soil

Heavy metals	Co	Cr	Cu	Ni	Pb	Zn
Permissible limit[a]	N/A	N/A	135–270	75–150	250–500	300–600
Permissible limit[b]	50	150	140	100	300	300
Uncontaminated soil[c]	N/A	5–3000	2–100	10–1000	2–200	10–300

N/A not available

[a]Bureau of Indian Standards; [b]European Union Standards; [c]Bowen (1966)

In the contour map of Pb (Fig. 14), local anomaly, i.e. exceeding threshold limit (> 38 ppm) is noticed in the southern part of the area, over the lateritic soil of Bolgarh Formation. Concentration of Pb is less over laterite and Gorumahisani Group of rocks which indicates that it is enriched in felsic igneous rocks relative to mafic rocks. Though Pb is a potentially hazardous element, there is no threat to environment and living organisms as it occurs less than the permissible limit (Table 7) in the study area.

Figure 15 shows higher values of Zn in the southeastern and northeastern parts over the Eastern Ghat Supergroup of rocks and meta-sedimentaries of Gorumahisani Group. The uniform distribution of medium concentration in the entire area may be partly attributed to the lithology and partly to anthropogenic activity, i.e. agriculture. However, since there is no Pb anomaly associated with Zn anomaly, its enrichment is due to use of Zn in fertilizers for increasing crop productivity. Zinc is an essential trace element for humans,

animals and plants (Micó et al. 2006). It is used as fertilizer to increase the crop yield and quality production.

Trace metals (e.g. Co and Zn) even in low concentrations have serious health effects as they are non-biodegradable and persistent in nature (Khan et al. 2010; Duruibe et al. 2007; Ikeda et al. 2000). Trace elements (< 0.01%) find their way into the animal body either by direct absorption, via air and water, or food chain. Thus, even a small additional pollution component can pose a serious health problem under some circumstances though the hazardous impacts of these elements are dependent upon the period of exposure, concentration and quantity of material used (Gupta 1999). As the elements discussed above are of high concentrations above permissible limit as given in Table 7 (Chauhan 2014; Mushtaq and Khan 2010; Kabata-Pendias and Pendias 2001; EU 2002; Awashthi 2000; Bowen 1966) in some parts of the study area their mobility, bioavailability, speciation and other physico-chemical characteristics needs to be studied in detail to know about the possible health and environmental hazards.
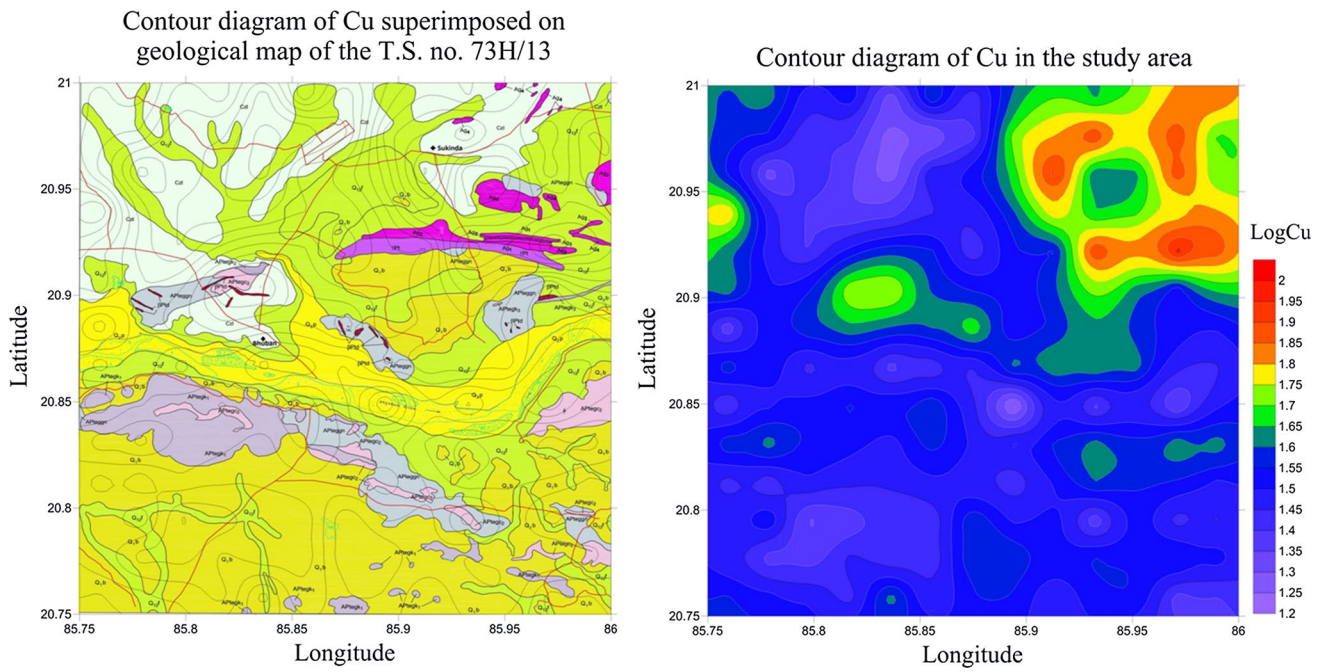
Contour diagram of Cu superimposed on
geological map of the T.S. no. 73H/13

Contour diagram of Cu in the study area

Fig. 13 Contour diagram of Cu in the study area

Contour diagram of Pb superimposed on
geological map of the T.S. no. 73H/13
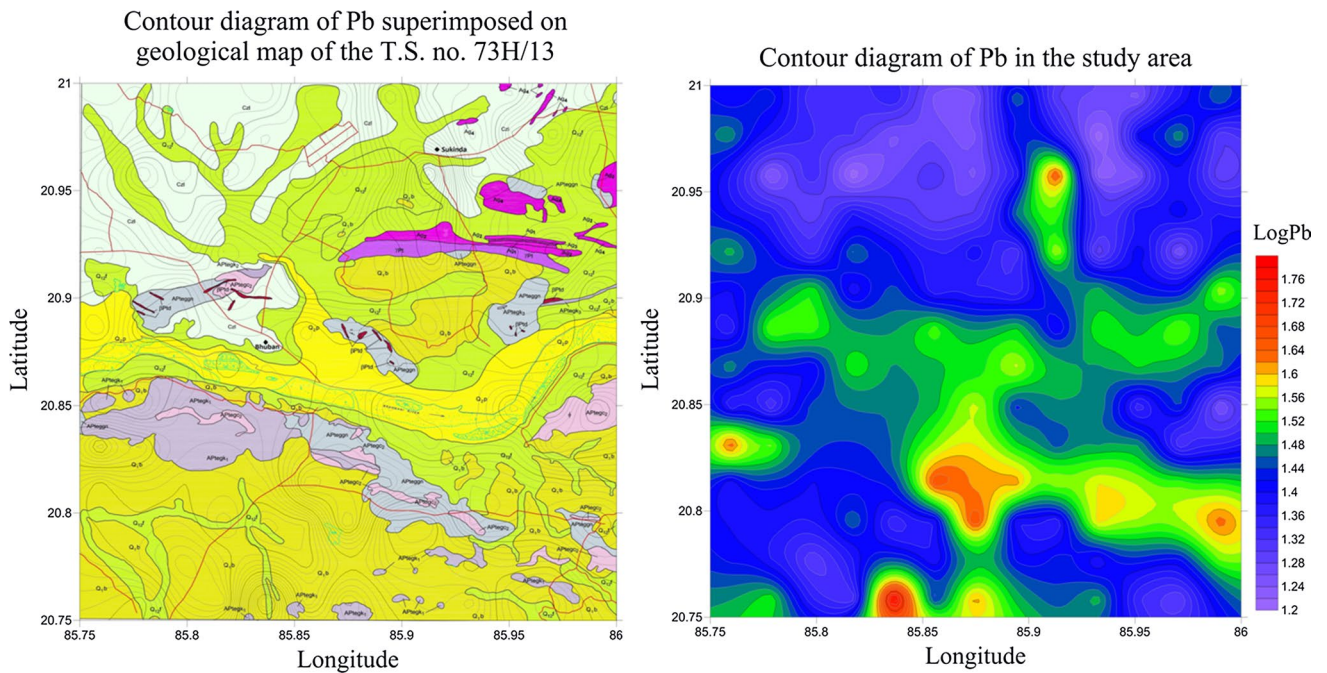
Contour diagram of Pb in the study area

Fig. 14 Contour diagram of Pb in the study area

Conclusion

The geochemical maps show clear images of the geochemical landscape and element distributions and can serve as basis for future studies and investigations in the study area. This study also shows that the elemental geochemical survey of the country India, currently in progress will produce a database that will have much wider applications than conventional mineral exploration and geological
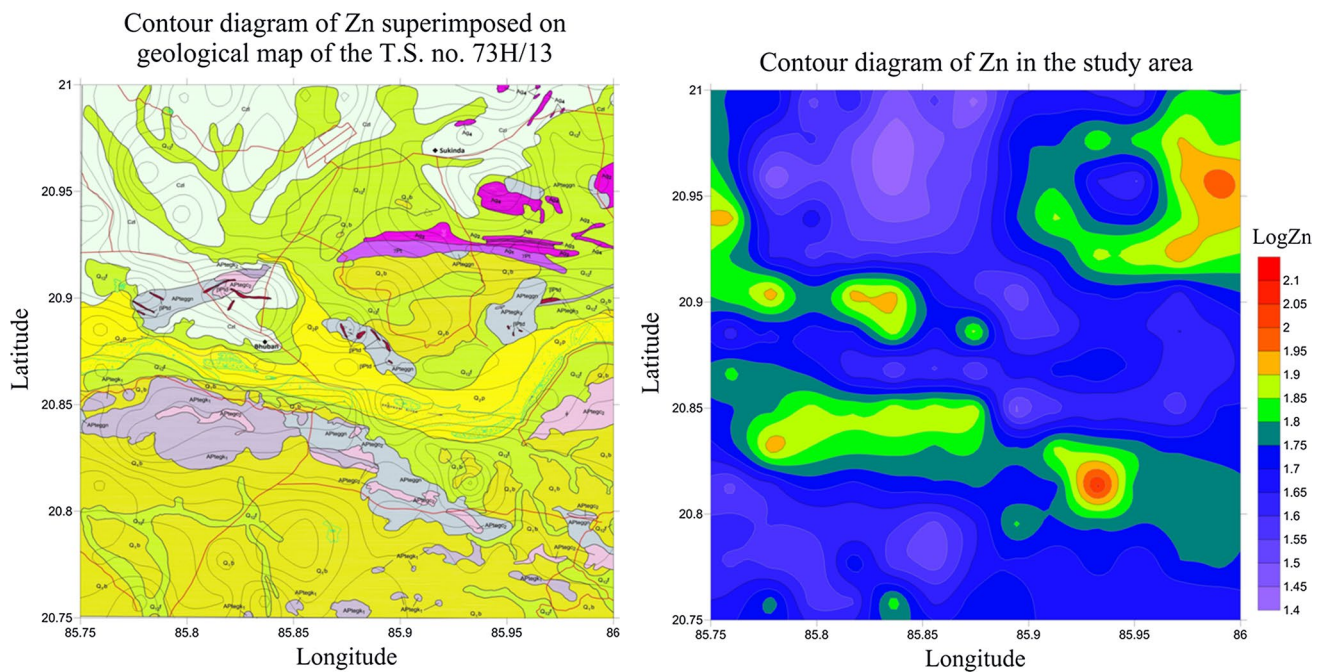
Fig. 15 Contour diagram of Zn in the study area

mapping. From the above discussion, it is inferred that detailed investigation may be required in order to delineate the potential zones for most pronounced Cr and Ni in northwestern and northeastern parts of the area. Lateritic terrain with higher values of Cr and Ni indicates the occurrence of mafic or ultramafic bodies lying underneath. Health and agricultural authorities need to take actions in the high and low anomalous regions of the heavy metals of their interest for the betterment of the environment and society.

References

Adekeye KS (2012) Modified simple robust control chart based on median absolute deviation. Int J Stat Probab 1(2):91–95. https://doi.org/10.5539/ijsp.v1n2p91

Appleton JD, Ridgway J (1992) Regional geochemical mapping in developing country and its application to environmental studies. Appl Geochem Suppl 2:103–110

Awashthi SK (2000) Prevention of Food Adulteration Act no 37 of 1954. Central and state rules as amended for 1999, 3rd edn. Ashoka Law House, New Delhi

BI (2007) The world's worst polluted places, the top ten of the dirty thirty. Blacksmith Institute, New York, pp 16–17

Bowen HJM (1966) Trace elements in biochemistry. Academic Press, New York. Recited from Sharma RK, Agrawal M, Marshall F (2007) Heavy metal contamination of soil and vegetables in suburban areas of Varanasi, India. Ecotoxicol Environ Saf 66:258–266

Chauhan G (2014) Toxicity study of metal contamination on vegetables grown in the vicinity of cement factory. Int J Sci Res Publ 4(11):1–8

Darnley AG, Bjiirklund A, Belviken B, Gustavsson N, Koval PV, Plant JA, Steenfelt A, Tauchid M, Xuejing X (1995) with contributions by Garrett RG, Hall GEM, A global geochemical database for environmental and resource management. UNESCO Publishing, Paris. ISBN 92-3-103085-X

Das AP, Mishra S (2010) Biodegradation of the metallic carcinogen hexavalent chromium Cr(VI) by an indigenously isolated bacterial strain. J Carcinog 9:6

Das S, Patnaik SC, Sahu HK, Chakraborty A, Sudarshan M, Thatoi HN (2013) Heavy metal contamination, physico-chemical and microbial evaluation of water samples collected from chromite mine environment of Sukinda, India. Trans Nonferr Met Soc China 23(2):484–493

Dhakate R, Singh VS, Hodlur GK (2008) Impact assessment of chromite mining on groundwater through simulation modeling study in Sukinda chromite mining area, Orissa, India. J Hazard Mater 160(2–3):535–547

Duruibe JO, Ogwuegbu MDC, Egwurugwu JN (2007) Heavy metal pollution and human biotoxic effects. Int J Phys Sci 2(5):112–118

Elliott AC, Woodward WA (2007) Statistical analysis quick reference guidebook with SPSS examples, 1st edn. Sage, London

EU (2002) European Union, heavy metals in wastes. European Commission on Environment. Recited from Chauhan G (2014) Toxicity study of metal contamination on vegetables grown in the vicinity of cement factory. Int J Sci Res Publ 4(11). ISSN 2250-3153

Field A (2009) Discovering statistics using SPSS, 3rd edn. Sage, London

Ghasemi A, Zahediasl S (2012) Normality tests for statistical analysis: a guide for non-statisticians.Int J Endocrinol Metab 10(2):486–489. https://doi.org/10.5812/ijem.3505

Gupta DC (1999) Environmental aspects of selected trace elements associated with coal and natural waters of Pench Valley coalfield of India and their impact on human health. Int J Coal Geol 40:133–149

Ikeda M, Zhang ZW, Shimbo S, Watanabe T, Nakatsuka H, Moon CS, Matsuda Inoguchi N, Higashikawa K (2000) Urban population exposure to lead and cadmium in east and south-east Asia. Sci Total Environ 249:373–384

Kabata-Pendias A, Pendias H (2001) Trace elements in soils and plants, 3rd edn. CRC Press, Boca Raton, p 413

Khan S, Rehman S, Khan AZ, Khan AM, Shah MT (2010) Soil and vegetables enrichment with heavy metals from geological sources in Gilgit, northern Pakistan. Ecotoxicol Environ Saf 73:1820–1827

Leys C, Ley C, Klein O, Bernard P, Licata L (2013) Detecting outliers: do not use standard deviation around the mean, use absolute deviation around the median. J Exp Soc Psychol 49(4):764–766

Licht OAB, Tarvainen T (1996) Multipurpose geochemical maps produced by integration of geochemical exploration data sets in The Paran Shield, Brazil. J Geochem Explor 56:167–182

MCD (2012) Compiled geological map of toposheet number 73H/13. Geological Survey of India, Map and Cartography Division, Eastern Region, Kolkata

Micó C, Peris M, Sánchez Recatalá L (2006) Heavy metal content of agricultural soils in a Mediterranean semiarid area: the Segura River Valley (Alicante, Spain). Span J Agric Res 4(4):363–372

Mohapatra S, Bohidar S, Pradhan N, Kar RN, Sukla LB (2007) Microbial extraction of nickel from Sukinda chromite overburden by *Acidithiobacillus ferrooxidans* and *Aspergillus* strains. Hydrometallurgy 85(1):1–8

Morrison JM, Goldhaber MB, Ellefsen KJ, Mills CT (2011) Cluster analysis of a regional-scale soil geochemical dataset in northern California. Appl Geochem 26:S105–S107

Mushtaq N, Khan KS (2010) Heavy metals contamination of soils in response to wastewater irrigation in Rawalpindi region. Pak J Agric Sci 47(3):215–224

NGCM SOP (2011) Standard operating procedure for national geochemical mapping. Geological Survey of India, Central Head Quarter, Kolkata

Odokuma-Alonge O, Adekoya JA (2013) Factor analysis of stream sediment geochemical data from onyami drainage system, Southwestern Nigeria. Int J Geosci 4(3):656–661. https://doi.org/10.4236/ijg.2013.43060

Pallant J (2007) SPSS survival manual, a step by step guide to data analysis using SPSS for windows, 3rd edn. McGraw Hill, Sydney, pp 179–200

Parsa M, Maghsoudi A, Yousefi M, Sadeghi M (2016a) Recognition of significant multi-element geochemical signatures of porphyry Cu deposits in Noghdouz area, NW Iran. J Geochem Explor 165:111–124

Parsa M, Maghsoudi A, Yousefi M, Sadeghi M (2016b) Prospectivity modeling of porphyry-Cu deposits by identification and integration of efficient mono-elemental geochemical signatures. J Afr Earth Sc 114:228–241

Parsa M, Maghsoudi A, Yousefi M, Sadeghi M (2016c) Multifractal analysis of stream sediment geochemical data: implications for hydrothermal nickel prospection in an arid terrain, eastern Iran. J Geochem Explor. https://doi.org/10.1016/j.gexplo.2016.11.013

Parsa M, Maghsoudi A, Yousefi M, Carranza EJM (2017) Multifractal interpolation and spectrum–area fractal modeling of stream sediment geochemical data: implications for mapping exploration targets. J Afr Earth Sc 128:5–15

Pattnaik BK, Equeenuddin SM (2016) Potentially toxic metal contamination and enzyme activities in soil around chromite mines at Sukinda Ultramafic Complex, India. J Geochem Explor 168:127–136

Plant JA, Hale M (1994) Introduction: the foundations of modern drainage geochemistry. In: Hale M, Plant JA (eds) Drainage geochemistry, Handbook of exploration geochemistry, vol 6. Elsevier, Amsterdam

Plant J, Smith D, Smith B, Williams L (2001) Environmental geochemistry at the global scale. Appl Geochem 16:1291–1308

Reimann C, Filzmoser P (2000) Normal and lognormal data distribution in geochemistry: death of a myth. Consequences for the statistical treatment of geochemical and environmental data. Environ Geol 39:1001–1014

Reimann C, Filzmoser P, Garrett RG (2005) Background and threshold: critical comparison of methods of determination. Sci Total Environ 346:1–16

Samuel J, Paul ML, Pulimi M, NirmalaM J, Chandrasekaran N, Mukherjee A (2012) Hexavalent chromium bioremoval through adaptation and consortia development from Sukinda chromite mine isolates. Ind Eng Chem Res 51(9):3740–3749

Smith DB, Smith SM, Horton JD (2013) History and evaluation of national-scale geochemical data sets for the United States. Geosci Front 4:167–183

Srivastava, SC, Mohanty PK (2005) Progress report on tectonomagmatic evolution of rocks around Duburi, Jajpur and Dhenkanal district, Orissa. Geological Survey of India, Operation: Orissa, Eastern Region, Field season 1998–99

Srivastava SC, Mohanty PK (2007) An interim report on exploration for chromite in Kanchanbahali–Bhusal sector and Chandar sector in northern parts of Brahmani valley, Jajpur and Dhenkanal districts, Orissa, (E-I). Geological Survey of India, Operation: Orissa, Eastern Region, Field season 2002–03

Srivastava SC, Mohanty PK (2011) Progress report on the search for chromite around Maulabhanj and Tangeria, Dhenkanal district, Orissa (P-II). Geological Survey of India, Operation: Orissa, Eastern Region, Field season 2009–10

Templ M, Filzmoser P, Reimann C (2008) Cluster analysis applied to regional geochemical data: problems and possibilities. Appl Geochem 23:2198–2213

Webb J (1975) Environmental problems and the exploration geochemist. In Geochemical Exploration 1974. Proc. of the Fifth International Geochemical Exploration Symposium, Vancouver. In I.L. Elliott and K. Fletcher (Editors) Developments in Economic Geology. Vol. I. Elsevier. Amsterdam. Assoc Explor Geochem Spec Publ 2:5–17

XRF SOP (2010) Standard operating procedure for X-ray fluorescence spectrometer. Geological Survey of India, Central Head Quarter, Kolkata

Yap CK (2012) Application of factor analysis in geochemical fractions of heavy metals in the surface sediments of the offshore and intertidal areas of Peninsular Malaysia. Sains Malays 41(4):389–394

Zhang C, Manheim FT, Hinde J, Grossman JN (2005) Statistical characterization of a large geochemical database and effect of sample size. Appl Geochem 20:1857–1874

Zhizhong C, Xuejing X, Wensheng Y, Jizhou F, Qin Z, Jindong F (2014) Multi-element geochemical mapping in Southern China. J Geochem Explor 139:183–192